The University of Oklahoma

Discovering the Higgs Bosons of Minimal Supersymmetry with Tau Leptons and a Bottom Quark

Chung Kao[a,b], Duane A. Dicus[c], Rahul Malhotra[d] and Yili Wang[a]

[a]*Department of Physics and Astronomy,*
University of Oklahoma, Norman, OK 73019, USA
[b]*Stanford Linear Accelerator Center,*
2575 Sand Hill Road, Menlo Park, CA 94025, USA
[c]*Center for Particles and Fields, University of Texas, Austin, TX 78712, USA*
[d]*Department of Physics and Astronomy,*
University of Hawaii, Honolulu, HI 96822, USA

(Dated: November 1, 2007)

Abstract

We investigate the prospects for the discovery at the CERN Large Hadron Collider or at the Fermilab Tevatron of neutral Higgs bosons through the channel where the Higgs are produced together with a single bottom quark and the Higgs decays into a pair of tau leptons, $bg \to b\phi^0 \to b\tau^+\tau^-$, $\phi^0 = h^0, H^0, A^0$. We work within the framework of the minimal supersymmetric model. The dominant physics background from the production of $b\tau^+\tau^-$, $j\tau^+\tau^-$ $(j = g, u, d, s, c)$, $b\bar{b}W^+W^-$, $W + 2j$ and Wbj is calculated with realistic acceptance cuts and efficiencies. Promising results are found for the CP-odd pseudoscalar (A^0) and the heavier CP-even scalar (H^0) Higgs bosons with masses up to one TeV.

PACS numbers: 14.80.Cp, 14.80.Ly, 12.60.Jv, 13.85Qk

I. INTRODUCTION

In the minimal supersymmetric standard model (MSSM) [1], the Higgs sector has two doublets, ϕ_1 and ϕ_2, which couple to fermions with weak isospin $t_3 = -1/2$ and $t_3 = +1/2$ respectively [2]. After spontaneous symmetry breaking, there remain five physical Higgs bosons: a pair of singly charged Higgs bosons $H^\pm$, two neutral CP-even scalars H^0 (heavier) and h^0 (lighter), and a neutral CP-odd pseudoscalar A^0. The Higgs potential is constrained by supersymmetry such that all tree-level Higgs boson masses and couplings are determined by just two independent parameters, commonly chosen to be the mass of the CP-odd pseudoscalar (M_A) and the ratio of vacuum expectation values of the neutral Higgs fields ($\tan\beta \equiv v_2/v_1$).

At the CERN Large Hadron Collider (LHC), gluon fusion ($gg \to \phi$, $\phi = h^0, H^0$, or A^0) is the major source of neutral Higgs bosons in the MSSM for $\tan\beta$ less than about 5. If $\tan\beta$ is larger than 7, neutral Higgs bosons are dominantly produced from bottom quark fusion $b\bar{b} \to \phi$ [3–7]. Since the Yukawa couplings of $\phi b\bar{b}$ are enhanced by $1/\cos\beta$, the production rate of neutral Higgs bosons, especially the A^0 or the H^0, is enhanced at large $\tan\beta$.

Recently, it has been suggested that the search for a Higgs boson produced along with a single bottom quark with large transverse momentum (p_T), where the leading order subprocess is $bg \to b\phi$ [8–11], could be more promising than the production of a Higgs boson associated with two high p_T bottom quarks [10] where the leading order subprocess is $gg \to b\bar{b}\phi$ [3, 12–15]. This has already been demonstrated to be the case for the $\mu^+\mu^-$ decay mode of the Higgs bosons [16]. For a large value of $\tan\beta$, the $\tau^+\tau^-$ decay mode [17, 18] is also a promising discovery channel for the A^0 and the H^0 in the MSSM because the branching fraction for Higgs decay into tau leptons is greater by a factor of $(m_\tau/m_\mu)^2 \sim 286$. The downside is that unlike muons, tau leptons can only be observed indirectly via their hadronic or leptonic decay products.

In this article, we present the prospects of discovering the MSSM neutral Higgs bosons produced with a bottom quark via Higgs decay into tau pairs. We calculate the Higgs signal and the dominant Standard Model (SM) backgrounds with realistic cuts and efficiencies and evaluate the 5σ discovery contour in the ($M_A, \tan\beta$) plane for the LHC and for the Tevatron.

II. THE PRODUCTION CROSS SECTIONS AND BRANCHING FRACTIONS

We calculate the cross section at the LHC for $pp \to b\phi + X$ and at the Tevatron for $p\bar{p} \to b\phi + X$ ($\phi = H^0, h^0, A^0$) via $bg \to b\phi$ with the parton distribution functions of CTEQ6L1 [19]. The factorization scale is chosen to be $M_\phi/4$ [6, 20]. In this article, unless explicitly specified, b represents a bottom quark (b) or a bottom anti-quark ($\bar{b}$). The bottom quark mass in the $\phi b\bar{b}$ Yukawa coupling is chosen to be the next-to-leading order (NLO) running mass at the renormalization scale μ_R, $m_b(\mu_R)$ [21], and it is calculated with $m_b(\text{pole}) = 4.7$ GeV and NLO evolution of the strong coupling [22]. We have also taken the renormalization scale for the production processes to be $M_\phi/4$, which effectively reproduces the effects of next-to-leading order [10]. Therefore, we take the K factor to be one for the Higgs signal.

The cross section for $pp \to b\phi \to b\tau^+\tau^- + X$ can be thought of as the Higgs production cross section $\sigma(pp \to b\phi + X)$ multiplied by the branching fraction of the Higgs decay into tau pairs $B(\phi \to \tau^+\tau^-)$. When the $b\bar{b}$ mode dominates Higgs decays, the branching fraction of $\phi \to \tau^+\tau^-$ is about $m_\tau^2/(3m_b^2(M_\phi) + m_\tau^2)$ where $m_b(M_\phi)$, the running mass at the scale M_ϕ, is used in the decay rates. This results in a branching fraction for $A^0 \to \tau^+\tau^-$ of ~ 0.1

for $M_A = 100$ GeV. Thus for $\tan\beta \gtrsim 10$ and $M_A \gtrsim 125$ GeV, the cross section of bA^0 or that of bH^0 is enhanced by approximately $\tan^2\beta$ and the branching fraction of Higgs decay to tau pair is close to 10%.

III.   TAU DECAY AND IDENTIFICATION

Tau leptons can decay either purely leptonically, $\tau^- \to \ell^- \bar{\nu}_\ell \nu_\tau$, with a branching ratio of around 18% for each mode $l = e, \mu$, or they can decay into low-multiplicity hadronic states and a ν_τ with a branching ratio $\simeq 64\%$ [23]. Therefore, for a $\tau^+\tau^-$ pair, the most likely scenario is one decaying leptonically and the other hadronically, which has a combined branching ratio of 46%. Also, the presence of an isolated lepton in the final state is useful in triggering the event and reducing backgrounds. Hence, we use this "lepton + τ-jet" signature in our study.

We model hadronic tau decays as the sum of two-body decays into $\pi\nu_\tau$, $\rho\nu_\tau$ and $a_1\nu_\tau$ with branching ratios given in the literature [23]. The tau is assumed to be energetic enough that all its decay products emerge in approximately the same direction as the tau itself. This manifests itself in the so-called "collinear approximation" which we use for both leptonic and hadronic decays. The approximation is confirmed to be accurate by comparison with an exact matrix element simulation for tau decay.

In Figure 1, we present the transverse momentum distribution $(d\sigma/dp_T)$ for the bottom quark (b), or the lepton (ℓ) or the tau hadron (j_τ) from tau decays, for the Higgs signal $pp \to bA^0 \to b\tau^+\tau^- \to b\ell j_\tau + X$. In addition, we show the p_T distribution for b, ℓ, or j_τ from the SM background $bg \to b\tau^+\tau^-$ (Drell-Yan). We have required $p_T(b) > 10$ GeV and $|\eta_b| < 2.5$. The purpose of this figure is to show these cross sections before any other cuts have been applied.

The ATLAS collaboration has studied identification efficiencies of τ-jets in detail [24]. Based on this we use an overall efficiency of 26% over 1- and 3-prong decays with a corresponding cut, $p_T(h) > 40$ GeV for the hadron $h = \pi, \rho, a_1$. This also corresponds to a mistag efficiency of $1/400$ for non-τ (i.e. QCD) jets. Rejection of jets from b quarks is higher, with only 1 in 700 being mistagged as τs. The transverse momentum cut on the lepton from tau decay is weaker, with $p_T(\ell) > 20$ GeV. Both the hadron and lepton are required to be in the central rapidity region $|\eta| < 2.5$. The acceptance cuts as well as tagging and mistagging efficiencies for the Fermilab Tevatron will be discussed in Section VII.

IV.   HIGGS MASS RECONSTRUCTION

The Higgs mass can be reconstructed indirectly, using the collinear approximation for τ decay products and the missing transverse momentum 2-vector, $\not{p}_{\mathbf{T}}$. Taking x_ℓ, x_h to be the energy fractions carried away from the decays by the lepton and hadron respectively, we have:

$$(\frac{1}{x_\ell} - 1)\mathbf{p_T^\ell} + (\frac{1}{x_h} - 1)\mathbf{p_T^h} = \not{p}_{\mathbf{T}} \tag{1}$$

This yields two equations for x_ℓ and x_h which can be solved to reconstruct the two original τ 4-momenta $p_\tau^\mu = p_\ell^\mu/x_\ell$, p_h^μ/x_h. Thus $M_\phi^2 = (p_\ell/x_\ell + p_h/x_h)^2$. Physically we must have $0 < x_\ell, x_h < 1$, and this provides a further cut to reduce the background.
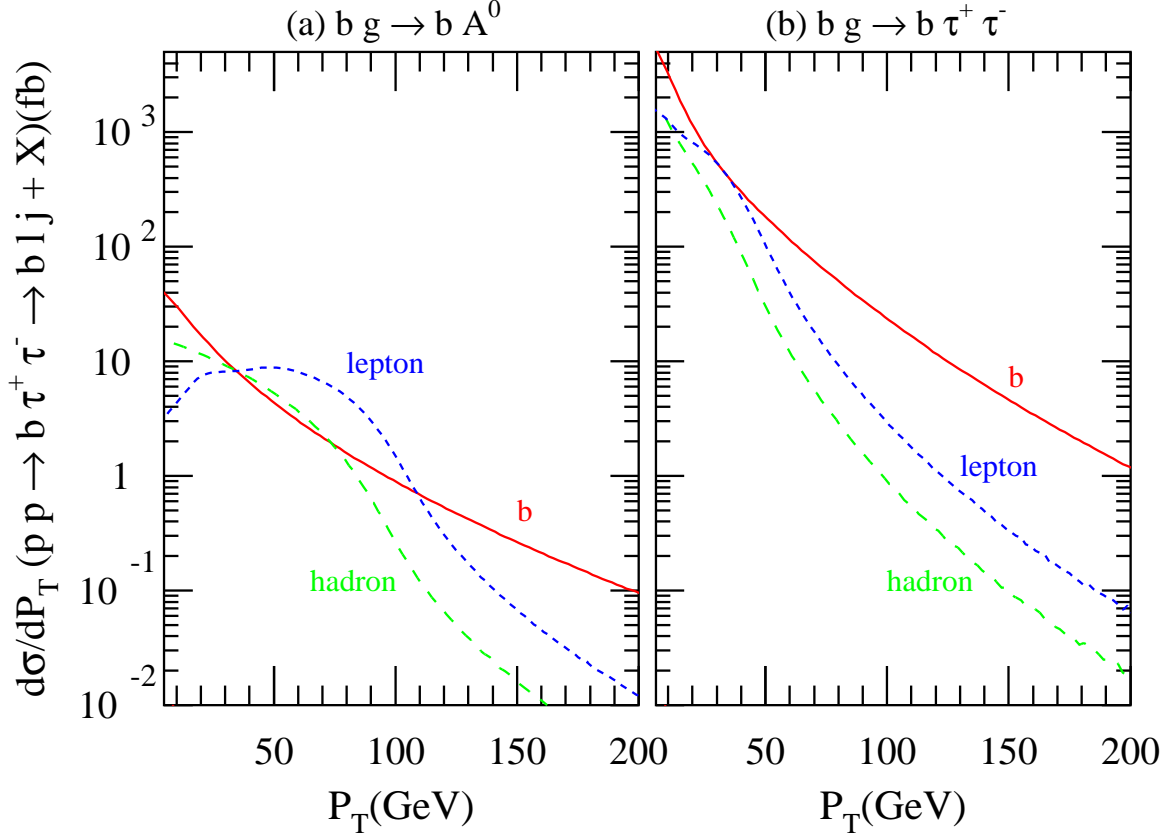
3

FIG. 1: The transverse-momentum distribution for (a) the Higgs signal from $bg \to bA^0 \to b\tau^-\tau^+ \to b\ell j + X$ with $M_A = 200$ GeV and $\tan\beta = 10$ as well as for (b) the physics background from $bg \to b\tau^-\tau^+ \to b\ell j + X, j = \pi, \rho$, or a_1. In the three curves, p_T refers to the transverse momentum of the b−quark or the lepton or the tau-jet.

Measurement errors in lepton and τ-jet momenta as well as missing transverse momentum give rise to a spread in the reconstructed mass about the true value. Based on the ATLAS and the CDF specifications we model these effects by Gaussian smearing of momenta:

$$\frac{\Delta E}{E} = \frac{0.50}{\sqrt{E}} \oplus 0.03 \tag{2}$$

for jets (with individual terms added in quadrature) and

$$\frac{\Delta E}{E} = \frac{0.25}{\sqrt{E}} \oplus 0.01 \quad \text{(LHC)} \tag{3}$$

$$\frac{\Delta E}{E} = \frac{0.15}{\sqrt{E}} \oplus 0.01 \quad \text{(Tevatron)} \tag{4}$$

for charged leptons.

We find that in more than 95% of the cases, the reconstructed mass lies within 15% of the actual mass. Therefore we apply a mass cut, requiring the reconstructed mass to lie in the mass window $M_\phi \pm \Delta M_{\tau\tau}$, where $\Delta M_{\tau\tau} = 0.15 M_\phi$ for an integrated luminosity (L) of 30 fb^{-1} and $\Delta M_{\tau\tau} = 0.20 M_\phi$ for $L = 300$ fb^{-1}. This cut is actually rather conservative because for larger Higgs masses, more than 90% of the reconstructed masses are within $5-10\%$ of

M_ϕ. We note that improvements in the discovery potential will be possible by narrowing $\Delta M_{\tau\tau}$ if the τ pair mass resolution can be improved.

Figure 2 shows the invariant mass distribution of the tau pair for the Higgs signal $pp \to bA^0 \to b\tau^+\tau^- + X$ via $bg \to bA^0$, and for the tau pair from the SM Drell-Yan background $bg \to b\tau^+\tau^-$. We have calculated the Higgs signal in two ways: (a) with the narrow width approximation

$$\sigma(pp \to bA^0 \to b\tau^+\tau^- + X) = \sigma(pp \to bA^0 + X) \times B(A^0 \to b\tau^+\tau^-)$$

and (b) the full calculation $\sigma(pp \to bA^0 \to b\tau^+\tau^- + X)$ with a Breit-Wigner resonance via $bg \to bA^0 \to b\tau^+\tau^-$. In this figure we have applied all acceptance cuts discussed in the next two sections except the requirement on invariant mass. We note that with energy-momentum smearing, the cross section in the narrow width approximation agrees very well with that evaluated for a Breit-Wigner resonance.
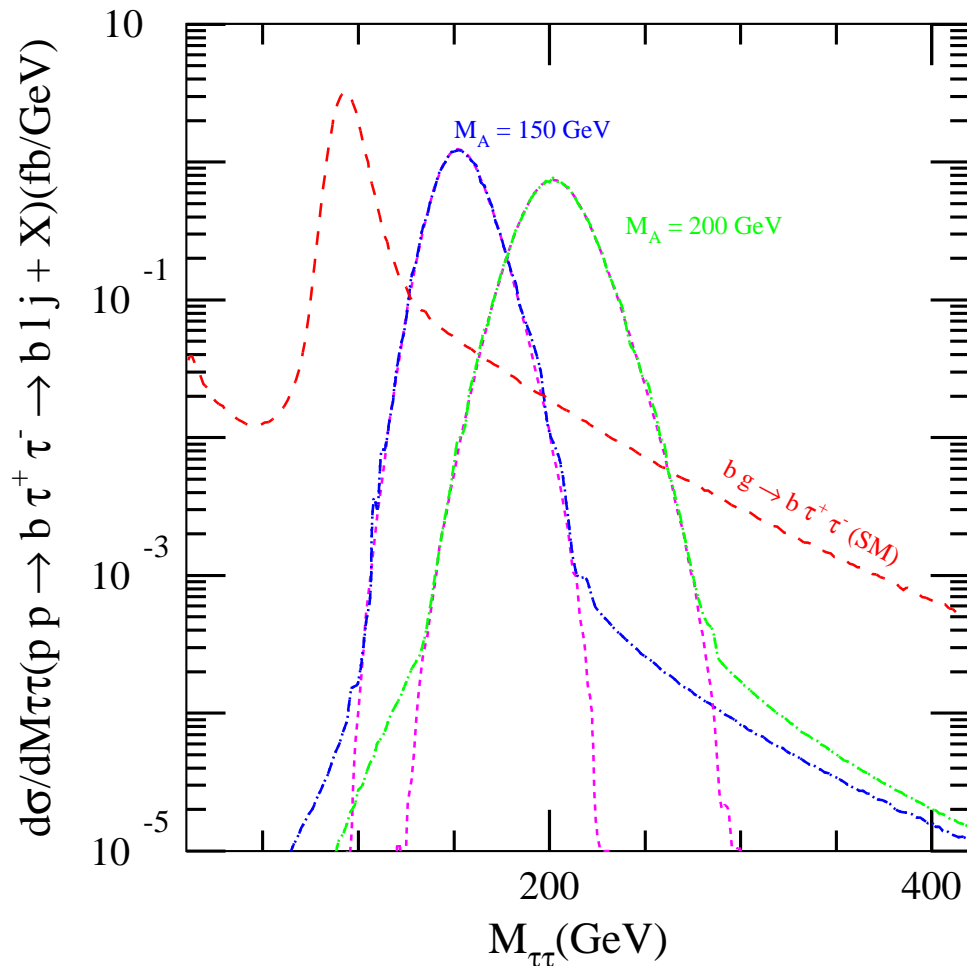

FIG. 2: The invariant-mass distribution distribution, $d\sigma/dM_{\tau\tau}(pp \to b\tau^+\tau^- \to b\ell j_\tau + \not{E}_T + X)$, for the Higgs signal from $bg \to bA^0 \to \tau^-\tau^+ \to b\ell j_\tau + X$ with $M_A = 150$ GeV or 200 GeV and $\tan\beta = 10$ as well as for the physics background from $bg \to b\tau^-\tau^+ \to b\ell j_\tau + X, j_\tau = \pi, \rho$, or a_1 (dash). We calculate the Higgs signal in the narrow width approximation (short dash) and with a Breit-Wigner resonance from a Higgs propagator (dash-dot).

V. THE PHYSICS BACKGROUND

From the above discussion, the signal we are looking for is b-jet (b) + lepton (ℓ) + τ-jet (j) + $\not{E}_T$ + X, where $\not{E}_T$ = missing transverse energy $\simeq \not{p}_T$ = missing transverse momentum. The dominant physics backgrounds to this final state come from:

(i) Drell-Yan processes: $pp \to jZ^*/\gamma^* + X \to j\tau^+\tau^- + X$, $j = u, d, s, c, b, g$. Approximately $60 - 70\%$ of the DY contribution arises from the subprocess $bg \to b\tau^+\tau^-$.

(ii) Top Production ($gg, q\bar{q} \to t\bar{t} \to b\bar{b}W^+W^-$): This can contribute in several ways depending on how the Ws decay. In order of highest to lowest importance, the relevant channels are the following. (a) $b\tau\nu b\ell\nu$: One W decays into $\tau\nu_\tau$ with the τ decaying hadronically while the other W provides $\ell\nu_\ell$. (b) $b\tau\nu b\tau\nu$: We can have both W's decaying into $\tau\nu_\tau$ with one tau decaying leptonically and the other hadronically. (c) $b\ell\nu bjj$: In this case we can have one W decay leptonically while the other W decays into jets ($W \to qq'$). We now have four possible jets in the final state i.e., 2 b's and $2j$ and one of them is tagged as a b quark while one of the other is mistagged as a τ-jet. (d) $b\ell\nu b\ell\nu$: We can have both Ws decay leptonically. Then we have two b quarks in the final state, one of them is tagged as a $b-$jet while the others is mistagged as a τ-jet. (e) $b\tau\nu bjj$: Finally we can have one W decay into $\tau\nu_\tau$ with the τ decaying leptonically while the other W decays into jets ($W \to qq'$). We now have four possible jets in the final state i.e., 2 b's and $2j$ and one of them is tagged as a b quark while one of the others is mistagged as a τ-jet.

(iii) tW Production ($bg \to tW \to bW^+W^-$): This is very similar to the top quark pair production just discussed. In order of decreasing importance, the relevant channels are as follows. (a) $b\tau\nu\ell\nu$: One W decays into $\tau\nu_\tau$ with the τ decaying hadronically while the other W provides $\ell\nu_\ell$. (b) $b\tau\nu\tau\nu$: We can have both W's decaying into $\tau\nu_\tau$ with one tau decaying leptonically and the other hadronically. (c) $b\ell\nu jj$: In this case we can have one W decay leptonically while the other W decays into jets ($W \to qq'$). We now have one b and $2j$ with one of the light quarks mistagged as a τ-jet. (d) $b\tau\nu jj$: Lastly we can have one W decay into $\tau\nu_\tau$ with the τ decaying leptonically while the other W decays into jets ($W \to qq'$). Again, we have one b and $2j$ with one of the light quarks mistagged as a τ-jet.

(iv) $W + 2j$ processes: $pp \to W + 2j + X$ with the subsequent decays $W \to \ell\nu_\ell; \ell = e, \mu$ or $W \to \tau\nu_\tau$ with the τ decaying leptonically. Here, one jet is tagged or mistagged as a b quark and the other mistagged as a τ-jet.

Due to the huge cross-section for $pp \to q\bar{q}g$ with $q = b, c$, it is also pertinent to check that heavy quark semi-leptonic decays such as $b \to cl\nu$ do not overwhelm the signal. We find that this background is effectively cut to less than 10% of the dominant background at all times by an isolation cut on the lepton $|\eta(\ell, j)| > 0.3$, the large rejection factor for non-τ jets, and the requirement $\not{E}_T > 20$ GeV.

For the lower integrated luminosity (L) of 30 fb^{-1}, we require $p_T(b, j) > 15$ GeV and $|\eta(b, j)| < 2.5$. The b-tagging efficiency (ϵ_b) is taken to be 60%, the probability that a c-jet is mistagged as a b-jet (ϵ_c) is 10% and the probability that any other jet is mistagged as a b-jet (ϵ_j) is taken to be 1%. For the higher luminosity $L = 300$ fb^{-1}, we take $\epsilon_b = 50\%$ and $p_T(b, j) > 30$ GeV [24].

In order to improve the signal significance we also apply a cut on the transverse mass of $m_T(\ell, \not{E}_T) < 30$ GeV. Using the definition of transverse mass given in [26] we find that this is very effective in controlling the $W + 2j$ and $t\bar{t}$ backgrounds. In addition we require $\phi(\ell, \tau - \text{jet}) < 170^o$, as suggested by ATLAS and CMS collaborations [24, 25], for the reconstruction of the Higgs mass as the invariant mass of tau pairs.

We have applied a K factor of 1.3 for the DY background [27], a K factor of 2 for $t\bar{t}$ [28], a K factor of 1.5 for tW [29], a K factor of 0.9 for $W + 2j$ [30], and a K factor of 2 for $bq \to Wbq, q = u, d, s, c$ [31] to include NLO effects. In order to further cut down the $t\bar{t}$ background, we apply a veto on events with more than 2 jets in addition to the b and τ jets. This is very effective because, in $t\bar{t} + X$ production, nearly 50% of events have at least one gluon from initial or final state radiation that passes $p_T > 15$ GeV and $|\eta| < 2.5$ [28]. Such events are then vetoed. We are also able to reduce contributions from top production where one $W \to jj$ decay occurs.

We have employed the programs MADGRAPH [32] and HELAS [33] to evaluate matrix elements for both signal and background processes.

VI.   THE DISCOVERY POTENTIAL AT THE LHC

Based on the cuts defined above we show in Figure 3 the signal and background cross sections for an integrated luminosity $L = 30$ fb^{-1} and $L = 300$ fb^{-1}. The signal is shown for $\tan\beta = 10$ and 50, with a common mass for scalar quarks, scalar leptons, gluino, and the μ parameter from the Higgs term in the superpotential, $m_{\tilde{q}} = m_{\tilde{g}} = m_{\tilde{\ell}} = \mu = 1$ TeV. All tagging efficiencies and K factors discussed above are included.

From this figure we note that the cross section of the Higgs signal with $\tan\beta \sim 50$ can be much larger than that of the physics background after acceptance cuts. The Drell-Yan processes make the major contributions to the physics background for Higgs mass $\lesssim 180$ GeV, but $t\bar{t}$ contributions become dominant for higher masses. The $W + 2j$ contribution is very effectively controlled by the b tagging requirement.

We define the signal to be observable if the lower limit on the signal plus background is larger than the corresponding upper limit on the background [34, 35], namely,

$$L(\sigma_s + \sigma_b) - N\sqrt{L(\sigma_s + \sigma_b)} > L\sigma_b + N\sqrt{L\sigma_b} , \tag{5}$$

which corresponds to

$$\sigma_s > \frac{N^2}{L}\left[1 + 2\sqrt{L\sigma_b}/N\right] . \tag{6}$$

Here L is the integrated luminosity, σ_s is the cross section of the Higgs signal, and σ_b is the background cross section. Both cross sections are taken to be within a bin of width $\pm\Delta M_{\tau\tau}$ centered at M_ϕ. In this convention, $N = 2.5$ corresponds to a 5σ signal. We take the integrated luminosity L to be 30 fb^{-1} and 300 fb^{-1} [24].

For $\tan\beta \gtrsim 10$, M_A and M_H are almost degenerate when $M_A \gtrsim 125$ GeV, while M_A and M_h are very close to each other for $M_A \lesssim 125$ GeV. Therefore, when computing the discovery reach, we add the cross sections of the A^0 and the h^0 for $M_A < 125$ GeV and those of the A^0 and the H^0 for $M_A \geq 125$ GeV [36].

Figure 4 shows the 5σ discovery contours for the MSSM Higgs bosons where the discovery region is the part of the parameter space above the curves. We have chosen $M_{\text{SUSY}} = m_{\tilde{q}} =$
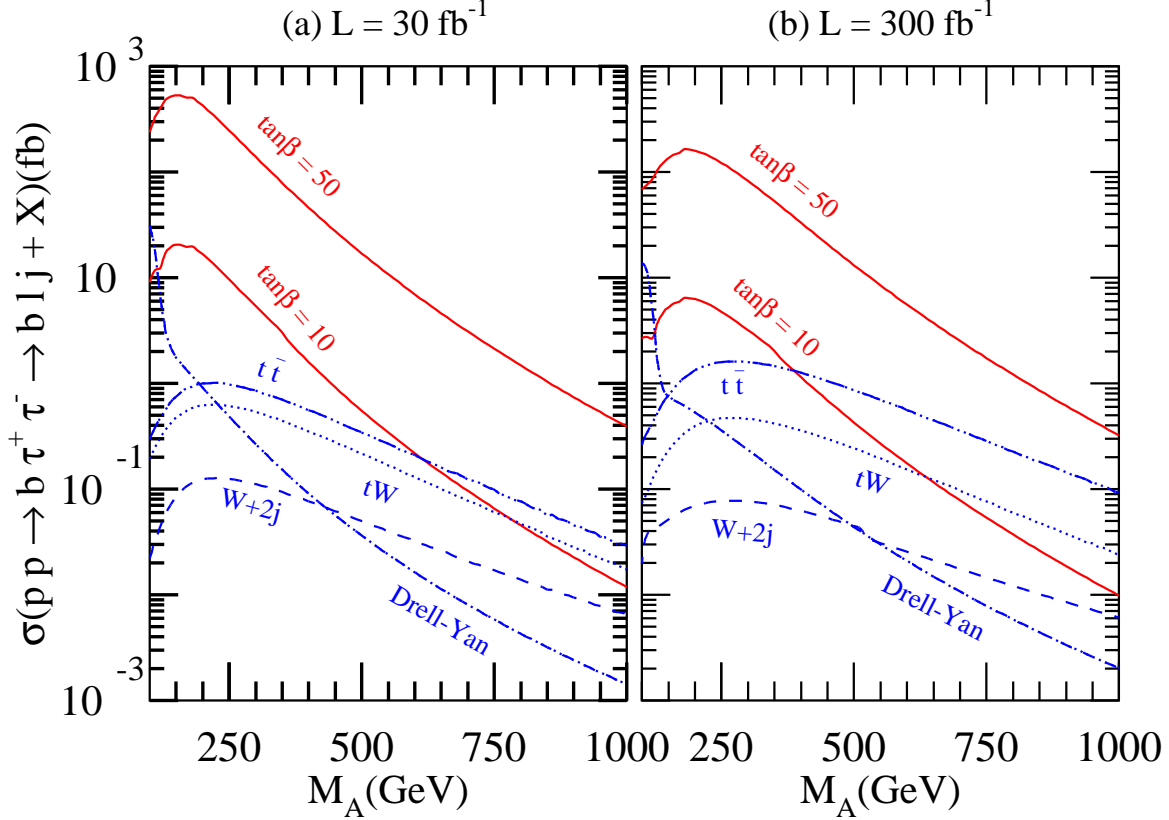
FIG. 3: The signal cross section at the LHC for luminosity $L = 30$ fb^{-1} and 300 fb^{-1}, as a function of M_A, and $\tan\beta = 10, 50$. Also shown are the background cross sections in the mass window of $M_A \pm \Delta M_{\tau\tau}$. We have applied K factors, acceptance cuts, and efficiencies of b, τ tagging and mistagging.

$m_{\tilde{g}} = m_{\tilde{\ell}} = \mu = 1$ TeV. If M_{SUSY} is smaller, the discovery region of $A^0, H^0 \rightarrow \tau^+\tau^-$ will be slightly reduced for $M_A \gtrsim 250$ GeV, because the Higgs bosons can decay into SUSY particles [37] and the branching fraction of $\phi \rightarrow \tau^+\tau^-$ is suppressed. For $M_A \lesssim 125$ GeV, the discovery region of $H^0 \rightarrow \tau^+\tau^-$ is slightly enlarged for a smaller M_{SUSY}, but the observable region of $h^0 \rightarrow \tau^+\tau^-$ is slightly reduced because the lighter top squarks make the H^0 and the h^0 lighter; also the $H^0 b\bar{b}$ coupling is enhanced while the $h^0 b\bar{b}$ coupling is reduced [36].

We find that the discovery contour even dips below $\tan\beta = 10$ for 100 GeV $< M_A <$ $300 - 400$ GeV depending on luminosity. Below $\tan\beta = 10$ our approximation of mass degeneracy of MSSM Higgs bosons breaks down; therefore we include only one Higgs boson (A^0) in our calculations.

VII. THE DISCOVERY POTENTIAL AT THE FERMILAB TEVATRON

To study the discovery potential of this channel at the Fermilab Tevatron Run II, we require

- one b quark with $p_T(b) > 15$ GeV, $|\eta(b)| < 2.5$ and a tagging efficiency $\epsilon_b = 60\%$,

- one isolated lepton with $p_T(\ell) > 10$ GeV and $|\eta(\ell)| < 2.0$,

8

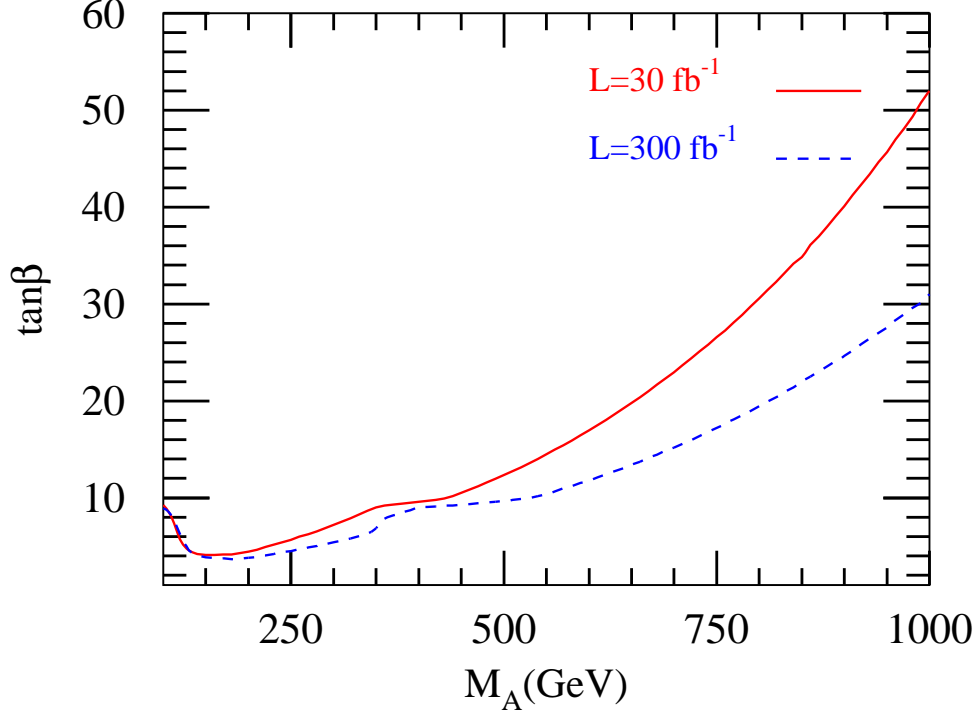FIG. 4: The 5σ discovery contours at the LHC for an integrated luminosity (L) of 30 fb^{-1}, and 300 fb^{-1} in the (M_A, $\tan\beta$) plane. The signal includes $\phi = A^0$ and h^0 for $M_A < 125$ GeV, and $\phi = A^0$ and H^0 for $M_A \geq 125$ GeV except that, for $\tan\beta < 10$, $\phi = A^0$ only. The discovery region is the part of the parameter space above the contours.

- one jet with $p_T(j) > 15$ GeV and $|\eta(j)| < 2.5$ for the tau jet, and a tagging efficiency of 38%,

- the transverse missing energy ($\not{E}_T$) should be greater than 20 GeV,

- the transverse mass of the lepton and missing transverse energy, $M_T(\ell, \not{E}_T)$, should be less than 30 GeV,

- the transverse angular separation of the lepton and tau jet, $\phi(\ell, j)$, should be less than 170°,

- the energy fractions for the lepton and the tau jet should be between 0 and 1, ($0 \leq x_\ell, x_h \leq 1$), and

- the invariant mass of the reconstructed tau pairs should be within the mass window of the Higg mass with $\Delta M_{\tau\tau} = 0.15 M_\phi$

In Figure 5 we show the signal and background cross sections for the Fermilab Tevatron. The signal is shown for $\tan\beta = 10$ and 50, with a common mass for scalar quarks, scalar leptons and the gluino $m_{\tilde{q}} = m_{\tilde{g}} = m_{\tilde{\ell}} = \mu = 1$ TeV. All tagging efficiencies and K factors discussed above are included.

From this figure we note that while $b\tau\tau$ and $t\bar{t}$ make major contributions to the physics background at the LHC, $b\tau\tau$ and Wjj become the dominant background at the Tevatron
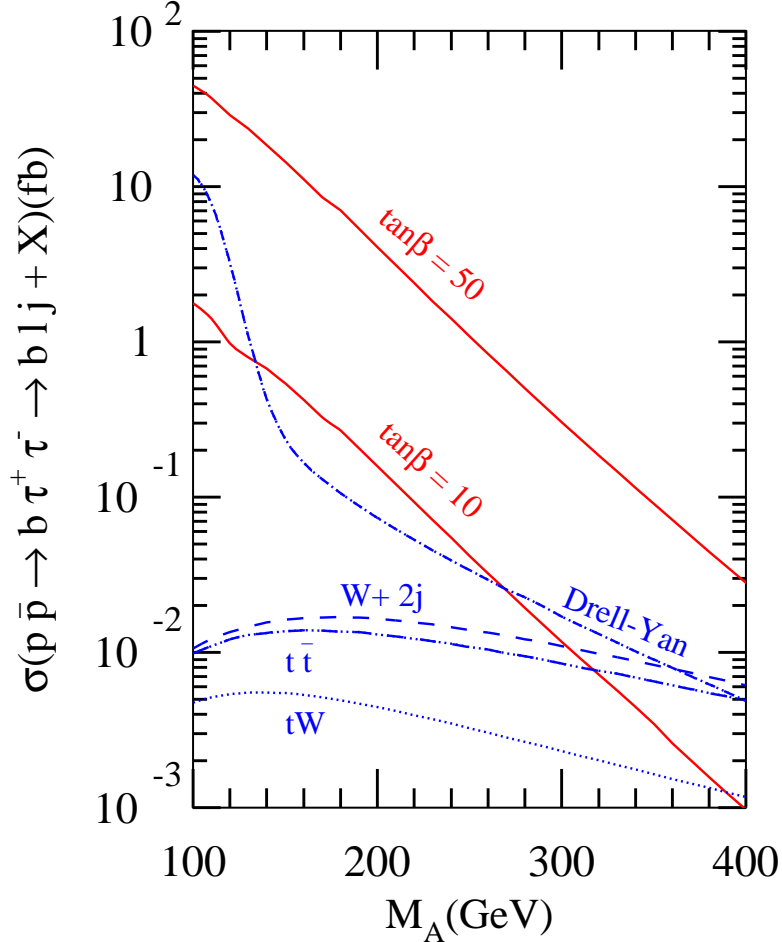
FIG. 5: The signal cross section at the Fermilab Tevatron Run II as a function of M_A, and $\tan\beta = 10, 50$. Also shown are the background cross sections in the mass window of $M_A \pm \Delta M_{\tau\tau}$. We have applied K factors, acceptance cuts, and efficiencies of b, τ tagging and mistagging.

for $M_A < 400$ GeV. The cross section of the Higgs signal with $\tan\beta \sim 50$ can be much larger than that of the physics background after acceptance cuts.

Figure 6 shows the 5σ discovery contours for the MSSM Higgs bosons where the discovery region is the part of the parameter space above the curves.

We find that the discovery contour for the Tevatron Run II can be slightly below $\tan\beta = 30$ with an integrated luminosity of 2 fb^{-1} and below $\tan\beta = 20$ with $L \simeq 8$ fb^{-1} for $M_A < 150$. For $\tan\beta \sim 50$, the Tevatron Run II will be able to discovery the Higgs bosons up to $M_A \sim 200$ GeV with $L = 2$ fb^{-1} and up to $M_A \sim 250$ GeV with $L \sim 8$ fb^{-1}.

VIII.   CONCLUSIONS

The tau pair decay mode is a promising channel for the discovery of the neutral Higgs bosons in the minimal supersymmetric model at the LHC. The A^0 and the H^0 should be observable in a large region of parameter space with $\tan\beta \gtrsim 10$. In particular, Fig. 4 shows that the associated final state of $b\phi \to b\tau^+\tau^-$ could discover the A^0 and the H^0 at the LHC with an integrated luminosity of 30 fb^{-1} if $M_A \lesssim 800$ GeV. At a higher luminosity of 300
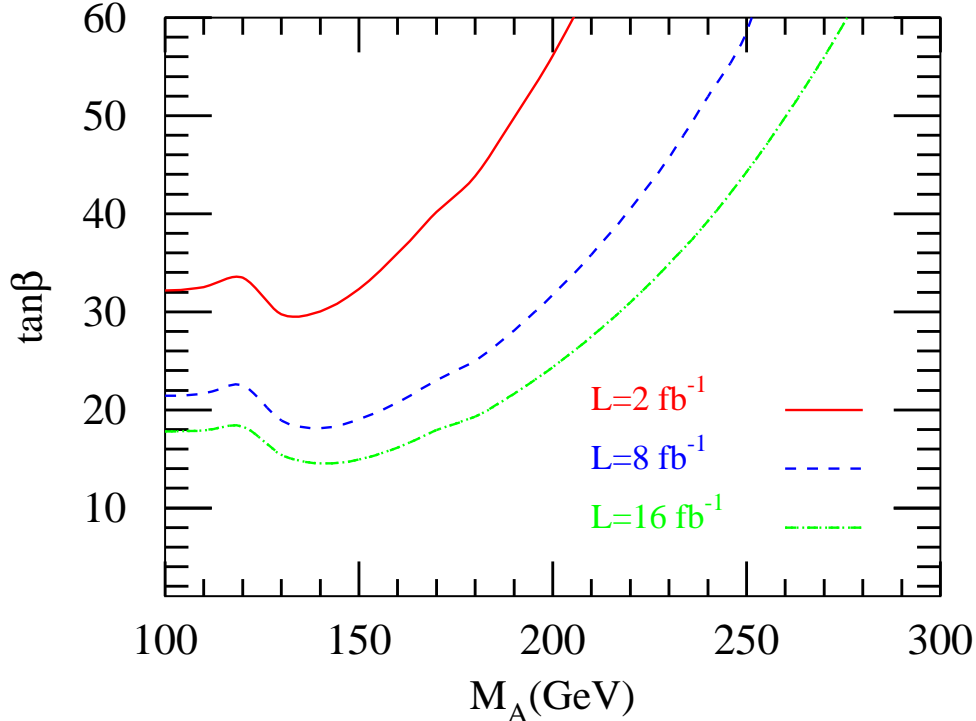
FIG. 6: The 5σ discovery contours at the Fermilab Tevatron Run II for an integrated luminosity (L) of 2 fb^{-1}, 8 fb^{-1}, 16 fb^{-1} in the M_A versus $\tan\beta$ plane. The signal includes $\phi = A^0$ and h^0 for $M_A < 125$ GeV, and $\phi = A^0$ and H^0 for $M_A \geq 125$ GeV except for $\tan\beta < 10$ where $\phi = A^0$ only. The discovery region is the part of the parameter space above the contours.

fb^{-1}, the discovery region in M_A is easily expanded up to $M_A = 1$ TeV for $\tan\beta \sim 50$.

In Figure 7, we compare the LHC discovery potential of $b\phi^0$ production for the muon pair discovery channel, as determined in Ref.[16], and the tau pair discovery channel, for an integrated luminosity of 30 fb^{-1}. It is clear that the tau pair channel can be discovered in a larger region of the parameter space. However, the muon pair channel can also be observable in a significantly large region. In addition, the muon pair channel will provide a good opportunity to precisely reconstruct the masses for MSSM Higgs bosons. The discovery of the associated final states of $b\phi \to b\tau^+\tau^-$ and $b\phi \to b\mu^+\mu^-$ will provide information about the Yukawa couplings of $b\bar{b}\phi$ and an opportunity to measure $\tan\beta$. The discovery of both $\phi \to \tau^+\tau^-$ and $\phi \to \mu^+\mu^-$ will allow us to study the Higgs Yukawa couplings with the leptons.

We find that the discovery contour for the Tevatron Run II can be slightly below $\tan\beta = 30$ with an integrated luminosity (L) of 2 fb^{-1} and below $\tan\beta = 20$ with $L \simeq 8$ fb^{-1} for $M_A < 150$. For $\tan\beta \sim 50$, the Tevatron Run II will be able to discover the Higgs bosons of MSSM up to $M_A \sim 200$ GeV with $L = 2$ fb^{-1} and up to $M_A \sim 250$ GeV with $L \sim 8$ fb^{-1}.

The inclusive tau pair channel ($\phi^0 \to \tau^-\tau^+$) has been studied by the ATLAS [18, 24] and the CMS [25] collaborations with realistic simulations. Both collaborations have confirmed that this channel will offer great promise at the LHC. Our results for $b\phi^0 \to b\tau^-\tau^+$ are consistent with those given in these references and also with the results of Ref. [38] for the Fermilab Tevatron.

11

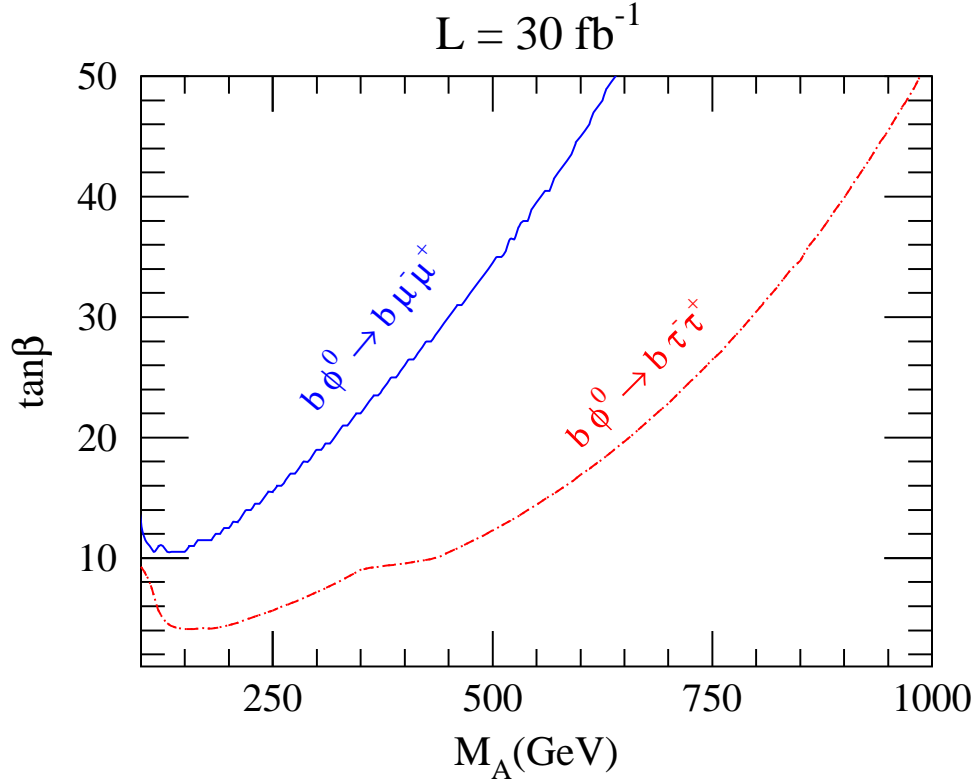FIG. 7: The 5σ discovery contours at the LHC for $b\phi^0 \to b\mu^-\mu^+$ and $b\phi^0 \to b\tau^-\tau^+$ with an integrated luminosity (L) of 30 fb^{-1}.

Acknowledgments

[1] H. P. Nilles, Phys. Rept. **110**, 1 (1984); H. E. Haber and G. L. Kane, Phys. Rept. **117**, 75 (1985).

[2] J. Gunion, H. Haber, G. Kane and S. Dawson, *The Higgs Hunter's Guide* (Addison-Wesley, Redwood City, CA, 1990).

[3] D. A. Dicus and S. Willenbrock, Phys. Rev. D **39**, 751 (1989).

[4] D. Dicus, T. Stelzer, Z. Sullivan and S. Willenbrock, Phys. Rev. D **59**, 094016 (1999).

[5] C. Balazs, H. J. He and C. P. Yuan, Phys. Rev. D **60**, 114001 (1999).

[6] F. Maltoni, Z. Sullivan and S. Willenbrock, Phys. Rev. D **67**, 093005 (2003).

[7] R. V. Harlander and W. B. Kilgore, Phys. Rev. D **68**, 013001 (2003).

[8] D. Choudhury, A. Datta and S. Raychaudhuri, arXiv:hep-ph/9809552.

[9] C. S. Huang and S. H. Zhu, Phys. Rev. D **60**, 075012 (1999).

[10] J. Campbell, R. K. Ellis, F. Maltoni and S. Willenbrock, Phys. Rev. D **67**, 095002 (2003).

[11] J. J. Cao, G. P. Gao, R. J. Oakes and J. M. Yang, Phys. Rev. D **68**, 075012 (2003).

[12] S. Dawson, D. Dicus and C. Kao, Phys. Lett. B **545**, 132 (2002).

[13] B. Plumper, DESY-THESIS-2002-005.

[14] S. Dittmaier, M. Kramer and M. Spira, arXiv:hep-ph/0309204.

[15] S. Dawson, C. B. Jackson, L. Reina and D. Wackeroth, arXiv:hep-ph/0311067.

[16] S. Dawson, D. Dicus, C. Kao and R. Malhotra, Phys. Rev. Lett. **92**, 241801 (2004) [arXiv:hep-ph/0402172].

[17] Z. Kunszt and F. Zwirner, Nucl. Phys. B **385**, 3 (1992).

[18] E. Richter-Was, D. Froidevaux, F. Gianotti, L. Poggioli, D. Cavalli and S. Resconi, Int. J. Mod. Phys. A **13**, 1371 (1998).

[19] J. Pumplin, D. R. Stump, J. Huston, H. L. Lai, P. Nadolsky and W. K. Tung, JHEP **0207**, 012 (2002).

[20] T. Plehn, Phys. Rev. D **67**, 014018 (2003).

[21] J. A. M. Vermaseren, S. A. Larin and T. van Ritbergen, Phys. Lett. B **405**, 327 (1997).

[22] W. J. Marciano, Phys. Rev. D **29**, 580 (1984).

[23] The Review of Particle Physics, S. Eidelman *et al.*, Phys. lett. B**592**, 1 (2004).

[24] ATLAS Collaboration, ATLAS Detector and Physics Performance Technical Design Report, CERN/LHCC 99-14/15 (1999).

[25] CMS Collaboration, D. Acosta et al., CMS Physics Technical Design Report, CERN/LHCC 2006-001 (2006).

[26] Collider Physics, V. Barger and R.J.N. Phillips, Redwood City, USA: Addison-Wesley (1987)

[27] J. Campbell, R. K. Ellis, F. Maltoni and S. Willenbrock, arXiv:hep-ph/0312024.

[28] R. Bonciani, S. Catani, M. L. Mangano and P. Nason, Nucl. Phys. B **529**, 424 (1998); P. Nason, S. Dawson and R. K. Ellis, Nucl. Phys. B **303**, 607 (1988).

[29] S. Zhu, Phys. Lett. B **524**, 283 (2002) [Erratum-ibid. B **537**, 351 (2002)].

[30] J. Campbell, R.K. Ellis and D. Rainwater, Phys. Rev. D **68**, 094021 (2003)

[31] J. Campbell, R. K. Ellis, F. Maltoni and S. Willenbrock, Phys. Rev. D **75**, 054015 (2007) [arXiv:hep-ph/0611348].

[32] MADGRAPH, by T. Stelzer and W.F. Long, Comput. Phys. Commun. **81**, 357 (1994).

[33] HELAS, by H. Murayama, I. Watanabe and K. Hagiwara, KEK report KEK-91-11 (1992).

[34] H. Baer, M. Bisset, C. Kao and X. Tata, Phys. Rev. D **46**, 1067 (1992).

[35] N. Brown, Z. Phys. C **49**, 657 (1991).

[36] M. Carena, J.R. Espinosa, M. Quiros and C.E.M. Wagner, Phys. Lett. B**355** 209 (1995); S. Heinemeyer, W. Hollik and G. Weiglein, Phys. Rev. D**58**, 091701 (1998).

[37] H. Baer, M. Bisset, D. Dicus, C. Kao and X. Tata, Phys. Rev. D **47**, 1062 (1993); H. Baer, M. Bisset, C. Kao and X. Tata, Phys. Rev. D **50**, 316 (1994).

[38] M. S. Carena, A. Menon, R. Noriega-Papaqui, A. Szynkman and C. E. M. Wagner, supersymmetric Phys. Rev. D **74**, 015009 (2006) [arXiv:hep-ph/0603106].